Supporting Information

NH_2-MIL-53(Al) Metal-Organic Framework as the Smart Platform for Simultaneous High-Performance Detection and Removal of Hg^{2+}

Liang Zhang,[a] Jing Wang,[a] Ting Du,[a] Wentao Zhang,[a] Wenxin Zhu,[a] Chengyuan Yang,[a] Tianli Yue,[a] Jing Sun,[b] Tao Li,[c] and Jianlong Wang[a,*]

[a] College of Food Science and Engineering, Northwest A&F University, 22 Xinong Road, Yangling 712100, Shaanxi, China.

[b] Qinghai Provincial Key Laboratory of Qinghai-Tibet Plateau Biological Resources, Northwest Institute of Plateau Biology, Chinese Academy of Sciences, 23 Xinning Road, Xining 810008, Qinghai, China.

[c] Shaanxi Institute for Food and Drug Control, Xi'an, 710065, China.

Corresponding author's E-mail: wanglong79@yahoo.com.

EXPERIMENTAL SECTION

Materials

Zirconium chloride ($ZrCl_4$), aluminum chloride hexahydrate ($AlCl_3 \cdot 6H_2O$), iron (III) chloride hexahydrate ($FeCl_3 \cdot 6H_2O$), chromic nitrate hydrate ($Cr(NO_3)_3 \cdot 9H_2O$), tetrabutyl titanate ($Ti(OC_4H_9)_4$), mercury nitrate ($Hg(NO_3)_2$) and 2-Aminoterephthalic acid (NH_2-H_2BDC) were obtained from Shanghai Aladdin Chemistry Co. Ltd. Sodium hydroxide (NaOH), N,N-Dimethylformamide (DMF) and absolute methanol were purchased from Sinopharm Chemical Reagent Co. Ltd. All reagents were of analytical grade and used as received without further purification. The distilled water was used throughout the experiment.

Synthesis of selected materials

The NH_2-MIL-53(Al), NH_2-MIL-101(Cr), NH_2-UiO-66(Zr), NH_2-MIL-88(Fe) and NH_2-MIL-125(Ti) were obtained based on the classical hydrothermal or solvothermal methods with partial modifications, respectively.

Synthesis of NH_2-MIL-53(Al). Typically, 0.543 g of NH_2-H_2BDC was dissolved in 30 mL of distilled water and was sonicated for 30 min. Then, 0.724 g of $AlCl_3 \cdot 6H_2O$ was added to the above solution and sonicated for another 30 min. The mixed solution was transferred into a 50 mL Teflon-lined autoclave and left to stand in an oven at 150 °C for 6 h. After cooling to room temperature, the obtained yellow precipitate was collected by centrifugation, which was washed three times with deionized water and DMF to remove unreacted components. The obtained solid was activated by stirring in absolute methanol for 24 h. Finally, the obtained precipitate was dried under vacuum at 70 °C for 12 h.

Synthesis of NH_2-UiO-66(Zr). 0.233 g of $ZrCl_4$ and 0.166 g of NH_2-H_2BDC were added to 33 mL of DMF solution containing 10% CH_3COOH, respectively. The above mixture was sonicated for 30 min at room temperature to obtain a homogeneous solution, which was then transferred to the 50 mL Teflon-lined autoclave and allowed to stand at 120 °C for 24 h. After hydrothermal treatment, the final product was filtered, washed with DMF and methanol. The obtained NH_2-UiO-66(Zr) was dried under vacuum at 60 °C for 12 h.

Synthesis of NH_2-MIL-88(Fe). Briefly, 0.374 g of $FeCl_3 \cdot 6H_2O$ and 0.251 g of NH_2-H_2BDC were completely dissolved in 30 mL of DMF by stirring treatment for 2 h. The obtained mixture solution was poured into a 50 mL Teflon-lined autoclave and then treated at 120 °C for 20 h. After cooling to ambient temperature, the brown suspension was filtered and was washed sequentially with DMF and ethanol. Finally, the prepared NH_2-MIL-88(Fe) was freeze-dried for 48 h.

Synthesis of NH_2-MIL-125(Ti). In detail, 1.8 mL of $Ti(OC_4H_9)_4$ and 1.36 g of NH_2-H_2BDC were added into a mixture solution containing 9 mL of DMF and 1 mL of dry methanol. The above mixture was stirred at room temperature for 1 h and was further treated at 150°C for 72 h in the Teflon-lined autoclave. After reaction, the bright yellow precipitate was collected by filtration, washed with DMF and methanol, respectively, which was dried under vacuum at 60 °C overnight to obtain the NH_2-MIL-125(Ti) powder.

Synthesis of NH_2-MIL-101(Cr). Typically, 1.6 g of $Cr(NO_3)_3 \cdot 9H_2O$ was added into 30 mL of distilled water containing 0.4 g NaOH and sonicated for 30 min. 0.72 g of NH_2-H_2BDC was then dissolved in the above mixture solution and sonicated for another 30 min. The mixed solution was transferred into 50 mL of Teflon-lined stainless steel autoclave and was maintained for 12 h at 150 ^oC. After natural cooling, the obtained mixture was collected by filtration and was washed three times with water, DMF and methanol, successively. The green product was dried under vacuum at 80 ^oC overnight.

Characterization

The images of SEM and elemental mapping were collected using a field emission scanning electron microscope (Hitachi S-4800) equipped with an EDAX energy dispersive detector. Powder X-ray diffraction (XRD) patterns were obtained by a powder diffractometer (Bruker D8 Advanced Diffractometer System) with a Cu Kα (1.5418 Å) source. Fourier-transform infrared (FT-IR) spectra were recorded from a Vetex70 spectrophotometer (Bruker Corp, Germany) using KBr pellets at ambient temperature. X-ray photoelectron spectroscopy (XPS) data were collected based on an Axis Ultra DLD X-ray photoelectron spectrometer equipped with an Al Kα X-ray source (1486.6 eV). Fluorescence spectra were were performed on a PE LS-55 spectrometer.

Fluorescence detection of Hg^{2+}

All fluorescence detection experiments of NH_2-MIL-53(Al) towards were carried out in aqueous solution at room temperature. 5 mg of NH_2-MIL-53(Al) particles was dissolved in 1L of deionized water followed by sonication for 10 minutes to obtain a homogeneous solution. The optimal excitation wavelength of the material was first determined by observing the intensity change of the emission peak.

The pH effect on the fluorescence intensity was also studied via monitoring the change in fluorescence intensity at different pH (1.0-7.0). To assess the stability of fluorescence, time-dependent fluorescence spectra were collected upon the dispersion of NH_2-MIL-53(Al) in water from 1 to 7 d. For the sensing detection towards Hg^{2+}, 500 μL of different concentrations of Hg^{2+} solution were added to 2 ml of the above stock solution so that final concentrations range is 1.0-997 μM. The fluorescence intensity of the stock solution mixed with Hg^{2+} was detected by an LS-55 spectrometer (PerkinElmer, Britain).

Furthermore, the fluorescence intensity changes of NH_2-MIL-53(Al) solutions treated with different metal ions were determined separately to explore the selectivity of NH_2-MIL-53(Al) towards Hg^{2+} detection. The anti-interference ability was also investigated. In detail, 2 times the concentration of various metal ions containing Li^+, Na^+, K^+, Ca^{2+}, Mg^{2+}, Ni^{2+}, Co^{2+}, Zn^{2+}, Pb^{2+}, Cd^{2+} and Mn^{2+} were added to the material solution containing 1 time of Hg^{2+}, and then the fluorescence change of the mixture was measured.

Adsorption experiments of Hg^{2+}

500 mg of NH_2-MIL-53(Al) powder was dissolved in 250 mg of deionized water and sonicated for 10 minutes to obtain a homogeneous stock solution (1 g L^{-1}). The solution pH was adjusted using 0.1 M HCl or 0.1 M NaOH in the pH range from 1.0 to 7.0. All adsorption-related experimental data were collected based on atomic fluorescence spectrometer (AFS-9330). The adsorption capacity was calculated according to eqn (1):

$$q_t = \frac{(C_0 - C_t)V}{m} \quad (1)$$

Where q_t is the amount of adsorption at time t, and C_0 represents the initial concentrations of Hg^{2+} (mg L^{-1}). C_t is the concentrations of Hg^{2+} at time t, V is volume of the reaction system (L), and m is the amount of adsorbent (g).

For adsorption kinetic experiments, 50, 100 and 300 mg L^{-1} of Hg^{2+} solution containing 0.25 g L^{-1} of NH_2-MIL-53(Al) were prepared separately in a 100 ml conical flask, which were placed in a shaker at 150 rpm and the residual concentration of Hg^{2+} at different time intervals (0-6 h) was measured by AFS. The obtained data was analyzed by different kinetic models including pseudo-first-order model, pseudo-second-order model and intra-particle diffusion model, and the consistent equations are described as follows:

$$\ln (q_e - q_t) = \ln q_e - k_1 t \quad (2)$$

$$\frac{t}{q_t} = \frac{1}{k_2 {q_e}^2} + \frac{t}{q_e} \quad (3)$$

$$q_t = k_i t^{1/2} + C_i \quad (4)$$

where q_e (mg g^{-1}) and q_t (mg g^{-1}) are the adsorption capacity at equilibrium and contact time t (min), respectively. k_1 (min^{-1}) represents the constant of the pseudo-first-order equation, which was determined by plotting $\ln(q_e-q_t)$ versus t. k_2 (g mg^{-1} min^{-1}), the rate constant of the pseudo-second-order model, was deduced from the intercept of the t/q_t versus t plot. C_i is the intercept of a plot of q_t versus t, and k_i (mg g^{-1} min^{-1}) represent the

intra-particle diffusion rate constant.

Furthermore, adsorption isotherm experiments were also carried out to describe the adsorption behavior. In detail, a series of concentration gradients (10-250 mg L^{-1}) of Hg^{2+} solution containing 0.25 g L^{-1} of material are prepared in a 10 ml centrifuge tube, and the above mixture was mixed in a shaker for 4 hours under different temperatures (25 °C, 35 °C and 45 °C). The residual Hg^{2+} concentration was detected by AFS. the Langmuir isotherm and Freundlich isotherm models were applied to explore the experimental data. The formulas of the two models are described as eqn (4) and (5) respectively.

$$\frac{C_e}{q_e} = \frac{1}{q_{max}k_L} + \frac{C_e}{q_{max}} \qquad (5)$$

$$q_e = k_F {C_e}^{1/n} \qquad (6)$$

where q_e (mg g^{-1}) represents the loading of Hg^{2+} at adsorption equilibrium, and q_{max} (mg g^{-1}) is the theoretical maximum adsorption capacity. C_e (mg L^{-1}) is the residual Hg^{2+} concentration at equilibrium. k_L (L mg^{-1}) represents the constant of the Langmuir model, which relates to the affinity and the binding energy of active site. k_F ($mg^{1-1/n}$ $L^{1/n}$ g^{-1}) and n represent the Freundlich isotherm constants, which correspond to the uptake capacity of the adsorbent and the adsorption intensity, separately. The recycling performance of was also studied, in which 0.1 M HCl solution containing 10% thiourea was formulated for use as the eluent.

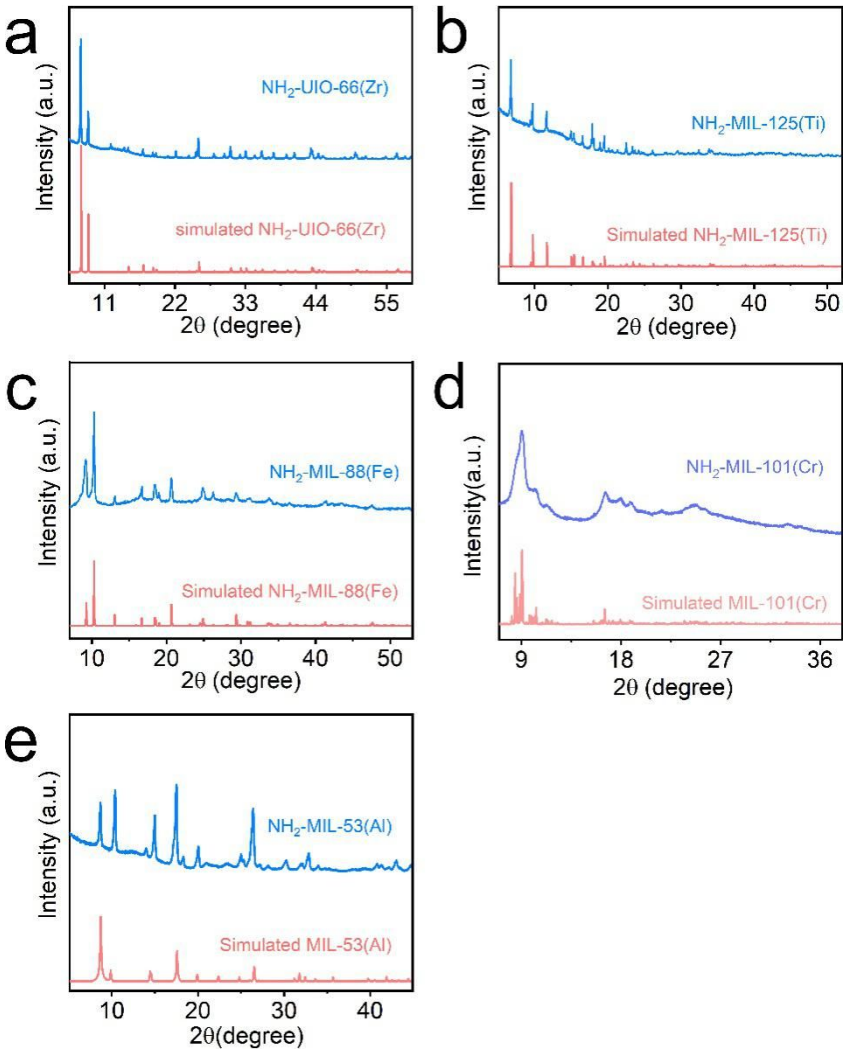

Figure S1. (a) XRD patterns of the NH_2-UIO-66(Zr) and simulated one. (b) XRD patterns of the NH_2-MIL-125(Ti) and simulated one. (c) XRD patterns of the NH_2-MIL-88(Fe) and simulated one. (d) XRD patterns of the NH_2-MIL-101(Cr) and simulated one. (e) XRD patterns of the obtained NH_2-MIL-53(Al) and simulated one.

Table S1. Fluorescence lifetime data of five selected MOF materials.

Samples	Compoment	Life time (ns)	B	X^2	Average Fluorescence Lifetime (ns)
NH_2-MIL-53(Al)	τ_1	0.6824	7186.879	1.214	9.57
	τ_2	4.1678	2236.622		
	τ_3	15.8027	952.369		
NH_2-UiO-66(Zr)	τ_1	0.5205	982.101	1.386	128.36
	τ_2	5.1993	13.578		
	τ_3	216.9276	3.854		
NH_2-MIL-88(Fe)	τ_1	1.6007	536.499	1.074	16.61
	τ_2	14.8419	8105.146		
	τ_3	23.2463	1462.158		
NH_2-MIL-101(Cr)	τ_1	15.1550	9833.697	1.209	15.59
	τ_2	55.0000	30.030		
NH_2-MIL-125(Ti)	τ_1	0.6442	6746.900	1.129	11.77
	τ_2	3.9582	1984.706		
	τ_3	15.3180	2016.779		

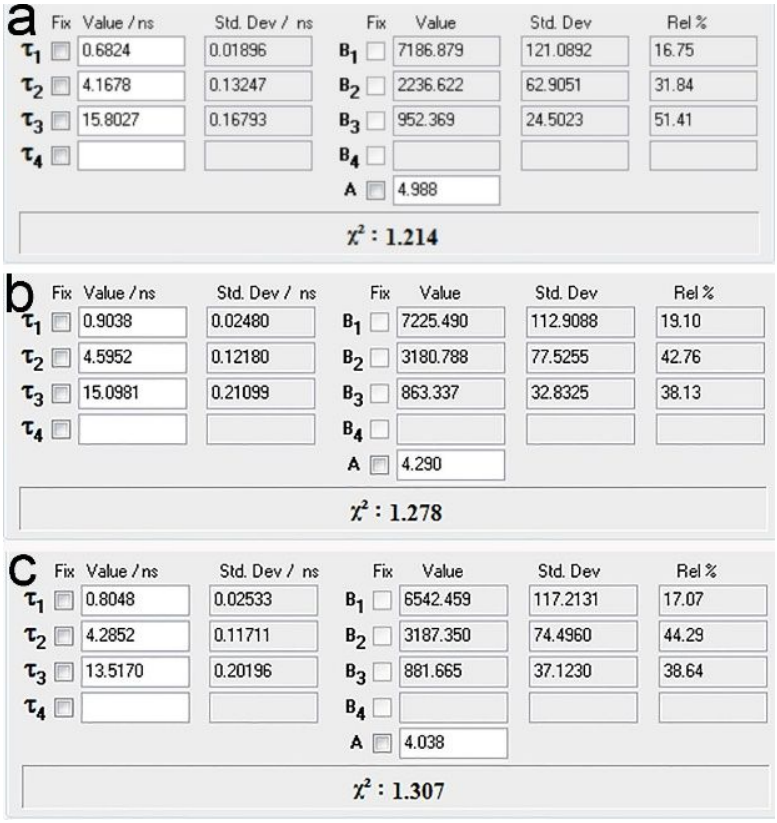

a

	Fix	Value / ns	Std. Dev / ns		Fix	Value	Std. Dev	Rel %
τ_1	☐	0.6824	0.01896	B_1	☐	7186.879	121.0892	16.75
τ_2	☐	4.1678	0.13247	B_2	☐	2236.622	62.9051	31.84
τ_3	☐	15.8027	0.16793	B_3	☐	952.369	24.5023	51.41
τ_4	☐			B_4	☐			
				A	☐	4.988		

χ^2 : 1.214

b

	Fix	Value / ns	Std. Dev / ns		Fix	Value	Std. Dev	Rel %
τ_1	☐	0.9038	0.02480	B_1	☐	7225.490	112.9088	19.10
τ_2	☐	4.5952	0.12180	B_2	☐	3180.788	77.5255	42.76
τ_3	☐	15.0981	0.21099	B_3	☐	863.337	32.8325	38.13
τ_4	☐			B_4	☐			
				A	☐	4.290		

χ^2 : 1.278

c

	Fix	Value / ns	Std. Dev / ns		Fix	Value	Std. Dev	Rel %
τ_1	☐	0.8048	0.02533	B_1	☐	6542.459	117.2131	17.07
τ_2	☐	4.2852	0.11711	B_2	☐	3187.350	74.4960	44.29
τ_3	☐	13.5170	0.20196	B_3	☐	881.665	37.1230	38.64
τ_4	☐			B_4	☐			
				A	☐	4.038		

χ^2 : 1.307

Table S2. The average fluorescence lifetime values of NH_2-MIL-53(Al) in the presence of different concentrations of Hg^{2+} : (a) The average lifetime values of NH_2-MIL-53(Al) without Hg^{2+}; (b) and (c) The average lifetime values of NH_2-MIL-53(Al) with Hg^{2+} (20 ppm and 40 ppm).

Table S3. The parameters of pseudo-first-order kinetic, pseudo-second-order kinetic, and intraparticle diffusion kinetic of Hg^{2+} adsorption.

C ($mg\ L^{-1}$)	Pseudo-first-order			Pseudo-second-order		
	$q_{e,c}$ ($mg\ g^{-1}$)	K_1	R^2	$q_{e,c}$ ($mg\ g^{-1}$)	K_2	R^2
10	53.10±1.07	4.14×10^{-5}	0.5274	55.56±0.65	0.0213	0.9982
100	86.90±1.15	2.46×10^{-5}	0.5272	89.77±0.44	0.0135	0.9978
300	137.87±1.01	2.43×10^{-5}	0.5880	143.06±0.76	0.0071	0.9930

C ($mg\ L^{-1}$)	Intraparticle diffusion model		
	K_i ($mg\ g^{-1}h^{-0.5}$)	C_i	R^2
10	0.21±0.02	52.21±0.02	0.9753
100	0.22±0.06	86.01±0.49	0.6700
300	0.38±0.07	136.38±0.70	0.7203

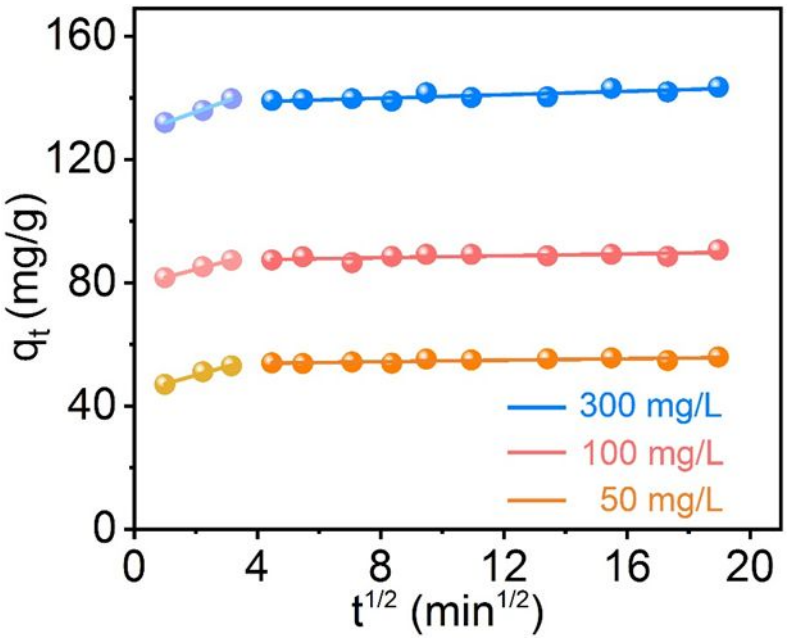

Figure S2. The fitting curves of intra-particle diffusion model of Hg^{2+} adsorption.

Table S4. The parameters of Langmuir model and Freundlich model of Hg^{2+} adsorption

T/K	Langmuir isotherm			Freundlich isotherm		
	q_m (mg g^{-1})	K_L (L mg^{-1})	R^2	K_f ($mg^{1+n}L^{-n}g^{-1}$)	n	R^2
298	88.11±5.56	0.056±0.014	0.9634	16.144±2.32	3.060±0.32	0.9133
308	153.85±15.40	0.038±0.013	0.9434	21.115±1.83	2.669±0.15	0.8931
318	219.30±16.20	0.036±0.008	0.9946	26.327±4.05	2.496±0.23	0.8718

Table S5. Comparison of the Hg^{2+} adsorption properties of prepared NH_2-MIL-53(Al) with other materials reported in previous article.

Adsorbents	Sorption capacity (mg g^{-1})	Reference
RB-KCC-1	115.5	1
Nin-NH-MIL-101(Al)	127.4	2
QDs-MMS-Rh6G	17.7	3
MIL-101-Thymine	51.3	4
Thiol-modified biochars	126.6	5
Fe_3O_4@Chitosan-pSDCalix	86.7	6
Starch/SnO_2 nanocomposite	192.0	7
Hg-PET-TSC	137.1	8
GOMNP	16.6	9
$\{[Ni_{1.5}(L)(NH_2\text{-bpy})\text{-}(H_2O)]\cdot 7.5H_2O\}_n$	93.7	10
HMSMCs-A	118.6	11
NH_2-MIL-53(Al)	153.8	This work

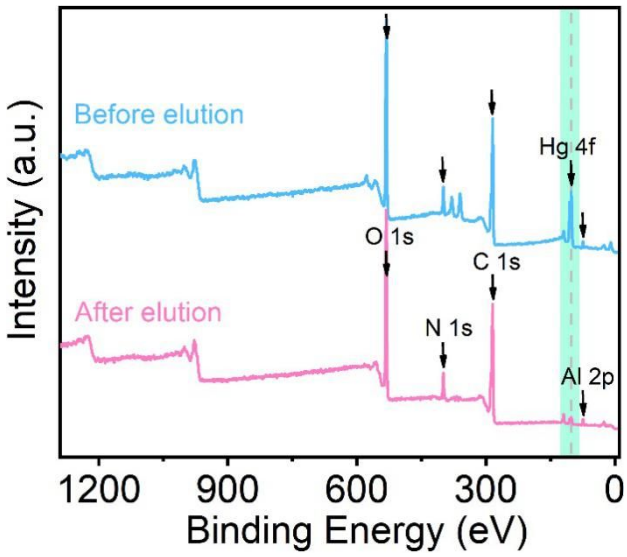

Figure S3. XPS survey spectra of Hg^{2+}-loaded NH_2-MIL-53(Al) before and after elution.

Table S6. Changes in the elements of the Hg^{2+}-loaded NH_2-MIL-53(Al) before and after elution.

Elements	Area(s)					Hg (%)
	C	N	O	Al	Hg	
Before elution	416898.83	86768.07	565583.66	16342.77	238939.75	0.18
After elution	416466.59	77564.6	531034.02	16614.94	25631.27	0.02

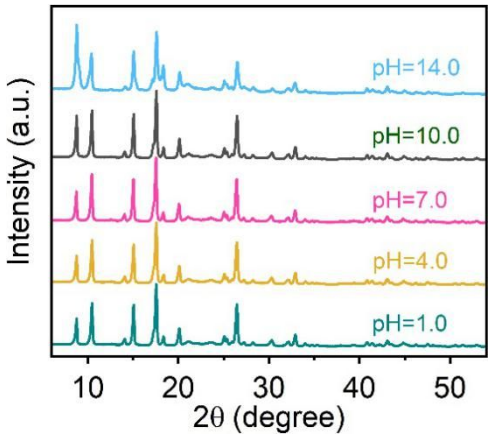

Figure S4. XRD patterns of NH_2-MIL-53(Al) at different pH conditions.

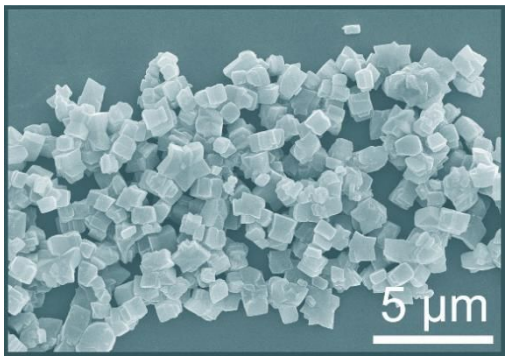

Figure S5. Overall SEM image of NH_2-MIL-53(Al) after Hg^{2+} adsorption.

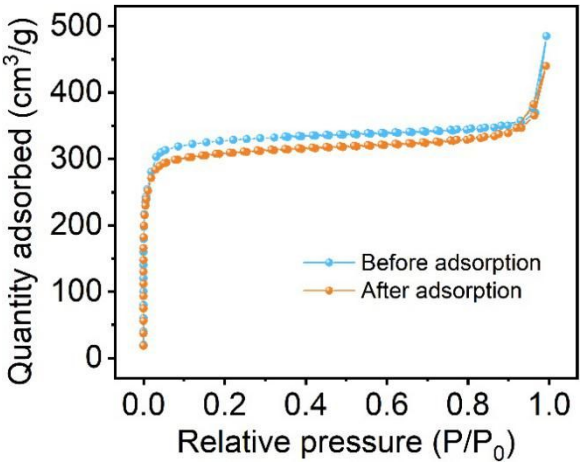

Figure S6. N_2 adsorption-desorption isotherms of NH_2-MIL-53(Al) before and after Hg^{2+} adsorption.

Table S7. Related data of N_2 adsorption-desorption isotherms of NH_2-MIL-53(Al) before and after Hg^{2+} adsorption.

	NH_2-MIL-53(Al)	
	S_{BET} (cm^2 g^{-1})	Pore Volume (cm^3 g^{-1})
Before adsorption	1347.83	0.75
After adsorption	1233.19	0.68

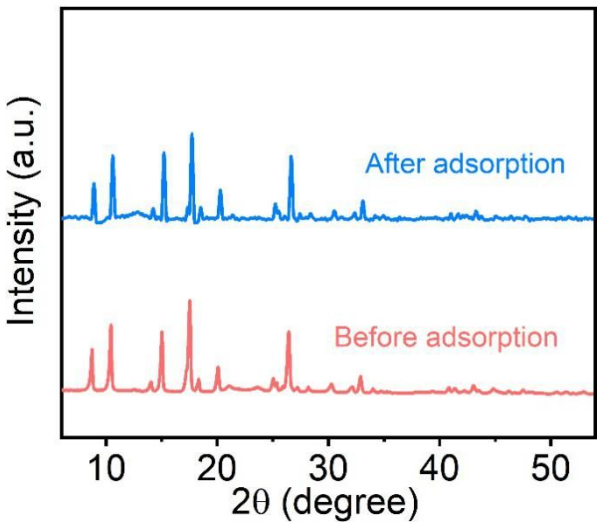

Figure S7. XRD patterns of NH_2-MIL-53(Al) before and after Hg^{2+} adsorption.

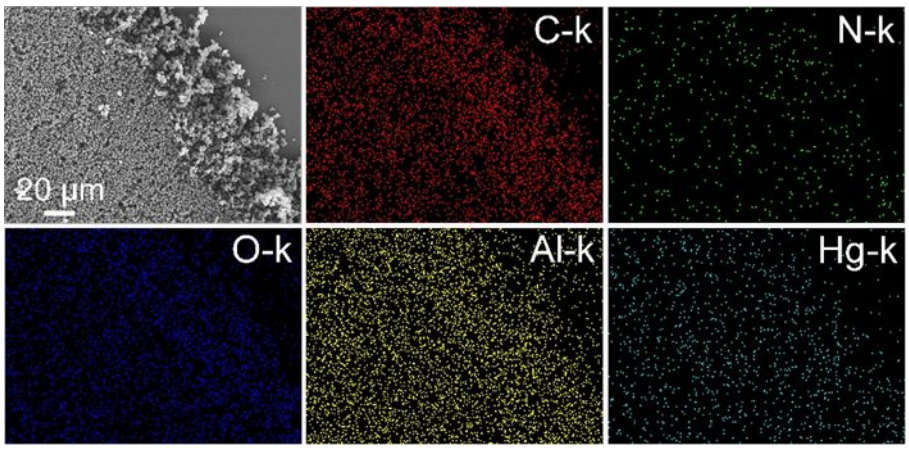

Figure S8. SEM-elemental mapping images of the C, N, O, Al and Hg in NH_2-MIL-53(Al) after Hg^{2+} adsorption.

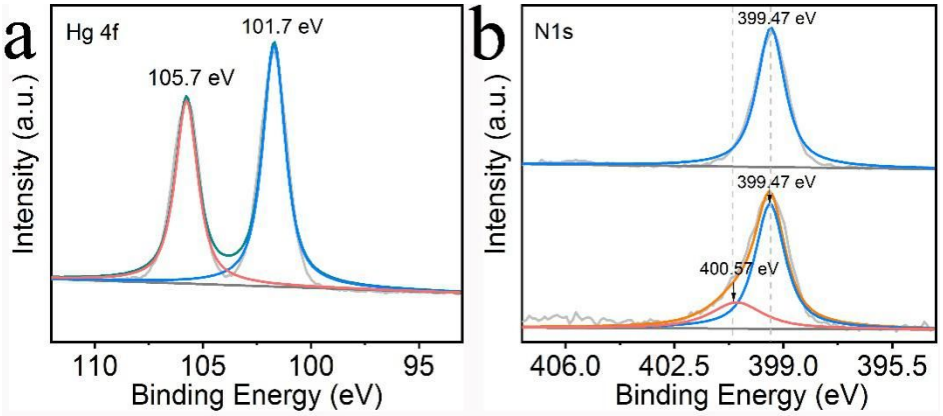

Figure S9. (a) XPS spectra of Hg 4f in NH_2-MIL-53(Al). (b) XPS spectra of N1s in amino group of NH_2-MIL-53(Al) before and after Hg^{2+} adsorption.

References

(1) Sun, Z. B.; Guo, D.; Zhang, L.; Li, H. Z.; Yang, B.; Yan, S. Q. Multifunctional Fibrous Silica Composite with High Optical Sensing Performance and Effective Removal Ability toward Hg^{2+} Ions. *J. Mater. Chem. B*. **2015**, *3*, 3201-3210.

(2) Shahat, A.; Elsalam, S, A,; Herrero-Martínez, J, M, Simó-Alfonso, E. F.; Ramis-Ramos, G. Optical Recognition and Removal of Hg(II) Using a New Self-Chemosensor Based on a Modified Amino-Functionalized Al-MOF. *Sens. Actuators B*. **2017**, *253*, 164-172.

(3) Wang, Y. Y.; Tang, M. M.; Shen, H.; Che, G. B.; Qiao, Y., Liu, B.; Wang, L. Recyclable Multifunctional Magnetic Mesoporous Silica Nanocomposite for Ratiometric Detection, Rapid Adsorption, and Efficient Removal of Hg (II). *ACS Sustainable Chem. Eng*. **2018**, *6*, 1744-1752.

(4) Luo, X. B.; Shen, T. T.; Ding, L., Zhong, W. P.; Luo, J. F.; Luo, S. L. Novel Thymine-Functionalized MIL-101 Prepared by Post-Synthesis and Enhanced Removal of Hg^{2+} from Water. *J. hazard. Mater.* **2016**, *306*, 313-322.

(5) Huang, Y.; Xia, S. Y.; Lyu, J. J.; Tang, J. C. Highly Efficient Removal of Aqueous Hg^{2+} and CH_3Hg^+ by Selective Modification of Biochar with 3-Mercaptopropyltrimethoxysilane.*Chem. Eng. J.* **2019**, *360*, 1646-1655.

(6) Bhatti, A. A.; Oguz, M.; Yilmaz, M. One-Pot Synthesis of Fe_3O_4@ Chitosan-pSDCalix Hybrid Nanomaterial for the Detection and Removal of Hg^{2+} Ion from Aqueous Media. *Appl. Surf. Sci.* **2018**, *434*, 1217-1223.

(7) Naushad, M.; Ahamad, T.; Sharma, G.; Ala'a, H.; Albadarin, A. B.; Alam, M. M.; ALOthman, Z. A.; Alshehri, S. M.; Ghfar, A. A. Synthesis and Characterization of a New Starch/SnO_2 Nanocomposite for Efficient Adsorption of Toxic Hg^{2+} Metal Ion. *Chem. Eng. J.* **2016**, *300*, 306-316.

(8) Monier, M.; Abdel-Latif, D. A. Synthesis and Characterization of Ion-Imprinted Chelating Fibers Based on PET for Selective Removal of Hg^{2+}. *Chem. Eng. J.* **2013**, *221*, 452-460.

(9) Diagboya, P. N.; Olu-Owolabi, B. I.; Adebowale, K. O. Synthesis of Covalently Bonded Graphene Oxide-Iron Magnetic Nanoparticles and the Kinetics of Mercury Removal. *Rsc Adv.* **2015**, *5*, 2536-2542.

(10) Shao, Z. C.; Huang, C.; Dang, J.; Wu, Q.; Liu, Y. Y.; Ding, J.; Hou, H. W. Modulation of Magnetic Behavior and Hg^{2+} Removal by Solvent-Assisted Linker Exchange Based on a Water-Stable 3D MOF. *Chem. Mater.* **2018**, *30*, 7979-7987.

(11) Zhang, X.; Wu, T. T.; Zhang, Y. X.; Ng, D. H. L.; Zhao, H. J.; Wang, G. Z. Adsorption of Hg^{2+} by Thiol Functionalized Hollow Mesoporous Silica Microspheres with Magnetic Cores. *Rsc Adv.* **2015**, *5*, 51446-51453.